

Functional Principal Component Analysis for Truncated Data

Caitrin Murphy^{1*}, Eric Laber^{1**}, Rhonda Merwin^{2***}, and Brian Reich^{3****}

¹ Department of Statistical Science, Duke University, Durham, North Carolina, U.S.A.

² Department of Psychiatry & Behavioral Sciences, Duke University, Durham, North Carolina, U.S.A.

³ Department of Statistics, North Carolina State University University, Raleigh, North Carolina, U.S.A.

**email*: caitrin.murphy@duke.edu

***email*: eric.laber@duke.edu

****email*: rhonda.merwin@duke.edu

*****email*: bjreich@ncsu.edu

SUMMARY: Functional principal component analysis (FPCA) is a key tool in the study of functional data, driving both exploratory analyses and feature construction for use in formal modeling and testing procedures. However, existing methods for FPCA do not apply when functional observations are truncated, e.g., the measurement instrument only supports recordings within a pre-specified interval, thereby truncating values outside of the range to the nearest boundary. A naïve application of existing methods without correction for truncation induces bias. We extend the FPCA framework to accommodate truncated noisy functional data by first recovering smooth mean and covariance surface estimates that are representative of the latent process's mean and covariance functions. Unlike traditional sample covariance smoothing techniques, our procedure yields a positive semi-definite covariance surface, computed without the need to retroactively remove negative eigenvalues in the covariance operator decomposition. Additionally, we construct a FPC score predictor and demonstrate its use in the generalized functional linear model. Convergence rates for the proposed estimators are provided. In simulation experiments, the proposed method yields better predictive performance and lower bias than existing alternatives. We illustrate its practical value through an application to a study with truncated blood glucose measurements.

KEY WORDS: Functional principal component analysis; Scalar-on-function regression; Truncated functional data; Truncated predictors.

1. Introduction

Functional data are inherently infinite-dimensional, so a finite approximation is required if trajectories are to be used as covariates in a regression, for missing trajectory prediction, or to analyze dominant modes of variation. Functional principal component analysis (FPCA) is a widely used dimension reduction technique that operates under the assumption that functional data are realizations of a L^2 process, characterized by continuous mean and covariance functions (Dauxois et al., 1982). Under this assumption, the Karhunen-Loève expansion permits centered functional trajectories to be expressed as infinite sums of eigenvectors and random FPC scores (Karhunen, 1946; Loève, 1946); each random score is a function of a centered realization from the L^2 process and an eigenfunction of the covariance surface. The FPCA literature is extensive for functional data observed with and without measurement error, as well as on sparse or dense time grids (e.g., Besse and Ramsay, 1986; James et al., 2000; Yao et al., 2005).

FPCA techniques are particularly applicable to regression. While mean and covariance functions offer information about the underlying functional process, the fraction of variance explained (FVE) interpretation of the random scores lends itself to scalar-on-function regression. The first use of the functional linear model (FLM) is credited to Ramsay and Dalzell (1991), and key extensions to the generalized functional linear model (GFLM) were made by Marx and Eilers (1999), James (2002), and Müller and Stadtmüller (2005). The Karhunen-Loève expansion allows the regression of a scalar-valued response on a functional predictor, with a corresponding L^2 coefficient, to be expressed as the regression of the response on an infinite sum of FPC scores and scalar-valued coefficients. Regularization can be achieved by truncating the functional covariate and coefficient FPC expansion to the first K terms that explain a pre-specified fraction of variance. This circumvents the need to add additional penalties, choose knot placement, or spline polynomial degree in advance (Morris, 2015).

While the class of techniques for analyzing functional data that are measured directly (or with additional error) is vast, the direct application of existing FPCA and scalar-on-function regression methods to data that are truncated is not immediate. Before continuing, it is important to highlight a key distinction in terminology. The word 'truncation' has previously been attached to scalar-on-function regression models for which functional covariates are assumed to influence the response on an unknown subset of the time domain (Hall and Hooker, 2016; Liu et al, 2022). In contrast, we use 'truncation' to mean instrument-induced truncation on the functional process. Interest in this setting is motivated by blood glucose data measured on a continuous glucose monitor (CGM) that only supports readings in the interval 40 – 400 mg/dL. The sensor imputes blood glucose levels outside of this range with the nearest boundary, thereby truncating the data. Systematic measurement truncation can also arise in other settings, notably from wearable technology (e.g., smartwatches) that provide continuous physiological monitoring information. The naïve application of existing methods to truncated functional data induces bias in the mean and covariance surface estimators, which propagates into the random FPC scores. For example, smoothing the sample mean in regions where trajectories are truncated from above potentially leads to the under-estimation of the mean function, and the over-estimation of the covariance function. A simple option is to treat truncated measurements as missing data, then take a complete case analysis approach and apply existing methods. However, removing truncated points, or truncated trajectories entirely, is inefficient and introduces unnecessary sparsity. Instead, we propose mean and covariance surface estimation procedures based on local log-likelihood maximization that utilize all of the data to recover the mean and covariance surfaces of the latent process; the truncation status and the behavior in neighboring regions are accounted for simultaneously. Our proposed method is also applicable to non-truncated data settings, particularly when the minimum eigenvalue of the sample covariance matrix is near zero.

Widespread covariance smoothing techniques pass the sample covariance estimate through a two-dimensional smoother (e.g., Yao et al., 2005; Rice and Silverman, 1991; Ramsay and Silverman, 2005), however, there is no guarantee that the eigenvalues of the smoothed surface are non-negative. Instead, we enforce a positive semi-definite (PSD) structure on the covariance surface during the estimation step to avoid this issue. In simulation experiments, the proposed mean and covariance estimation techniques exhibit less bias than current alternatives. Additionally, our suggested extensions to FPCA offer a solution to mitigate the bias incurred by using truncated functional data as regressors in a linear model. To the best of our knowledge, the impact of truncated regressors on linear models has only been studied for scalar-valued covariates by Rigobon and Stoker (2007, 2009), who noted that the replacement of truncated covariates with indicators is insufficient. We demonstrate the use of our proposed FPC score predictor in the GFLM and we derive convergence rates for the proposed estimators.

In Section 2, we provide a summary of the FPCA framework and its connection to scalar-on-function regression. In Section 3, we describe the estimation procedure for the mean and covariance functions, propose a FPC score predictor for truncated functional data, and derive convergence rates for the proposed functional linear model. Finite sample performance of the proposed surface estimators and FPC score predictor is evaluated through a simulation study in Section 4. In Section 5, a clinical application regarding the classification of eating disorders (EDs) from instrument-induced truncated blood glucose measurements is examined. Conclusions and limitations are discussed in Section 6.

2. Review of Functional Principal Component Analysis

We begin by introducing notation and briefly summarizing the FPCA framework for fully observed functional trajectories, measured with or without error, then we postulate a working GFLM with both functional and scalar-valued covariates. Suppose that there exists an

$L^2[0, 1]$ process, $Z(\cdot)$, with continuous mean and covariance functions defined by $\mu(t) = \mathbb{E}\{Z(t)\}$ and $\Sigma(s, t) = \text{Cov}\{Z(s), Z(t)\}$. All realizations $Z_i(\cdot)$ are assumed to be independent for $i = 1, \dots, n$. Application of Mercer's theorem yields the covariance operator decomposition $\Sigma(s, t) = \sum_{k \geq 1} \lambda_k \phi_k(s) \phi_k(t) \forall s, t \in [0, 1]$, where $\{\lambda_k, \phi_k(\cdot)\}_{k \geq 1}$ are the eigenpairs. Eigenvalues are ordered so that $\lambda_1 > \lambda_2 > \dots \geq 0$ and satisfy $\sum_{k=1}^{\infty} \lambda_k < \infty$; the eigenfunctions are orthonormal, i.e., $\int_0^1 \phi_k(t) \phi_j(t) dt = 1$ for $k = j$, and 0 otherwise. The k th FPC score for unit i is defined by

$$\xi_{i,k} = \int_0^1 \{Z_i(t) - \mu(t)\} \phi_k(t) dt, \quad (1)$$

and the Karhunen-Loève expansion allows each functional trajectory to be expressed as, $Z_i(t) = \mu(t) + \sum_{k \geq 1} \xi_{i,k} \phi_k(t)$, $\forall t \in [0, 1]$.

In the presence of measurement error, the noisy surrogate $\widetilde{W}_i(\cdot) = Z_i(\cdot) + \sigma(\cdot)\epsilon_i(\cdot)$ is observed for each unit i , where $\epsilon_i(\cdot)$ is a Gaussian white noise process, independent across subjects, with covariance operator $\Sigma_\epsilon(s, t) = 1$ if $s = t$ and 0 otherwise. The measurement error variance, $\sigma^2(\cdot)$, is assumed to be in $L^2[0, 1]$. Suppose each $\widetilde{W}_i(\cdot)$ is recorded at ordered times $\mathbf{T}_i = (T_{i,1}, \dots, T_{i,N_i})$; the number of recordings, N_i , and all elements in \mathbf{T}_i are random variables, thereby allowing for sparse and irregularly observed data. The number of measurements is assumed to be independent of observation times and measurements for each unit i , and the observation times are assumed to be iid; both assumptions are consistent with Yao et al. (2005). Noisy measurements from the latent process observed at times \mathbf{T}_i are denoted by $\widetilde{W}_i(\mathbf{T}_i) = \{\widetilde{W}_i(T_{i,1}), \dots, \widetilde{W}_i(T_{i,N_i})\}$. Similarly, we denote functions $\mu(\cdot)$, $\sigma^2(\cdot)$, and $\phi_k(\cdot)$ evaluated at \mathbf{T}_i by $\mu(\mathbf{T}_i)$, $\sigma^2(\mathbf{T}_i)$, and $\phi_k(\mathbf{T}_i) \in \mathbb{R}^{N_i}$, respectively. Define the $N_i \times N_i$ matrix $\widetilde{\Sigma}(\mathbf{T}_i, \mathbf{T}_i) = \Sigma(\mathbf{T}_i, \mathbf{T}_i) + \text{diag}\{\sigma^2(\mathbf{T}_i)\}$, with (j, k) th element equal to $\widetilde{\Sigma}(T_{i,j}, T_{i,k}) = \Sigma(T_{i,j}, T_{i,k}) + \sigma^2(T_{i,j})\mathbf{1}_{j=k}$. Estimating the FPC score from the noisy data is not immediate because a direct replacement of $Z_i(\cdot)$ with $\widetilde{W}_i(\cdot)$ in (1) will be biased. The seminal solution, proposed by Yao et al. (2005), uses the assumed joint

normality of the random scores and noisy data to construct the best linear unbiased predictor (BLUP) of the k th FPC score for unit i . The predictor for the k th FPC score for unit i is $\tilde{\xi}_{i,k} := \mathbb{E}\{\xi_{i,k} \mid \widetilde{W}_i(\mathbf{T}_i) = \tilde{w}_i(\mathbf{t}_i)\} = \lambda_k \phi_k(\mathbf{t}_i)^\top \widetilde{\Sigma}(\mathbf{t}_i, \mathbf{t}_i)^{-1} \{\tilde{w}_i(\mathbf{t}_i) - \mu(\mathbf{t}_i)\}$. An estimator of $\tilde{\xi}_{i,k}$ is given by $\widehat{\xi}_{n,i,k} := \widehat{\lambda}_{n,k} \widehat{\phi}_{n,k}(\mathbf{t}_i)^\top \widehat{\Sigma}_n(\mathbf{t}_i, \mathbf{t}_i)^{-1} \{\tilde{w}_i(\mathbf{t}_i) - \widehat{\mu}_n(\mathbf{t}_i)\}$, where $\widehat{\mu}_n(\mathbf{t}_i)$, $\widehat{\Sigma}_n(\mathbf{t}_i, \mathbf{t}_i)$, and $\{\widehat{\lambda}_{n,k}, \widehat{\phi}_{n,k}(\mathbf{t}_i)\}$ are estimators of $\mu(\mathbf{t}_i)$, $\widetilde{\Sigma}(\mathbf{t}_i, \mathbf{t}_i)$, and the k th eigenpair $\{\lambda_k, \phi_k(\mathbf{t}_i)\}$, respectively. Eigenpair estimates are obtained from an approximate discretization of the functional eigenequation for $\Sigma(\cdot, \cdot)$ (Ramsay and Silverman, 2005). In the following section, we discuss the utility of the FPC score estimates for modeling.

2.1 Scalar-on-Function Regression

In addition to the noisy functional measurements, suppose that p baseline covariates, $\mathbf{X}_i \in \mathbb{R}^p$, and an outcome, $Y_i \in \mathcal{Y}$, are recorded for each unit. The augmented data are of the form $[\{\widetilde{W}_i(\mathbf{T}_i), \mathbf{X}_i, Y_i\}]_{i=1}^n$ and the n copies are assumed to be iid. We assume that the conditional mean of the outcome given the latent functional process, $Z(\cdot)$, and the covariates, \mathbf{X} , is given by

$$\begin{aligned} g[\mathbb{E}\{Y_i \mid \mathbf{X}_i = \mathbf{x}_i, Z_i(\cdot) = z_i(\cdot)\}] &= \alpha_0 + \mathbf{x}_i^\top \boldsymbol{\alpha} + \int_0^1 z_i(t) \beta(t) dt \\ &= \alpha_0 + \mathbf{x}_i^\top \boldsymbol{\alpha} + \int_0^1 \mu(t) \beta(t) dt + \sum_{k \geq 1} \beta_k \xi_{i,k}, \end{aligned}$$

where $g(\cdot)$ is a link function, $\alpha_0 \in \mathbb{R}$ is the intercept, and $\boldsymbol{\alpha} \in \mathbb{R}^p$ is the vector of coefficients corresponding to the baseline covariates. The coefficient function $\beta(\cdot)$ weights the functional predictor across time and is assumed to be in $L^2[0, 1]$; the second equality follows from the expansion $\beta(t) = \sum_{k \geq 1} \beta_k \phi_k(t)$. As $Z(\cdot)$ is not directly observable, we reformulate the model in terms of the available data

$$\begin{aligned} &g[\mathbb{E}\{Y_i \mid \mathbf{X}_i = \mathbf{x}_i, \widetilde{W}_i(\mathbf{T}_i) = \tilde{w}_i(\mathbf{t}_i)\}] \\ &= g[\mathbb{E}\{g^{-1}(\alpha_0^* + \mathbf{x}_i^\top \boldsymbol{\alpha} + \sum_{k \geq 1} \beta_k \xi_{i,k}) \mid \mathbf{X}_i = \mathbf{x}_i, \widetilde{W}_i(\mathbf{T}_i) = \tilde{w}_i(\mathbf{t}_i)\}], \end{aligned}$$

which follows from the assumptions that (A1) $Y_i \perp \widetilde{W}_i(\cdot) \mid \{Z_i(\cdot), \mathbf{X}_i\}$, (A2) $Z_i(\cdot) \perp \mathbf{X}_i \mid \widetilde{W}_i(\cdot)$, (A3) $\alpha_0^* = \alpha_0 + \int_0^1 \mu(t)\beta(t)dt$, and (A4) FPC scores are independent across trajectories and uncorrelated across k , and each $\xi_{i,k} \sim \mathcal{N}(0, \lambda_k)$. The assumption of joint normality of the scores and $\widetilde{W}_i(\cdot)$ permits the direct evaluation of the expectation. In the following section, we extend the FPCA framework to accommodate truncated functional data, and illustrate the use of the FPC score predictors for modeling.

3. FPCA for Truncated Data

Instead of directly observing either $Z_i(\cdot)$ or $\widetilde{W}_i(\cdot)$, suppose we record a noisy surrogate truncated to the interval $[a, b]$, denoted by $W_i(\cdot)$. The truncated trajectory is given by $W_i(\cdot) = \max[a, \min\{b, \widetilde{W}_i(\cdot)\}]$. Define the truncation indicator matrix for unit i as $\mathbf{\Delta}_i(\mathbf{T}_i)$; rows are of the form $\mathbf{\Delta}_i(T_{i,j}) = (\delta_{i,j}^a, \delta_{i,j}^0, \delta_{i,j}^b)$, where $\delta_{i,j}^a = \delta_i^a(T_{i,j}) = \mathbf{1}\{\widetilde{W}_i(T_{i,j}) \leq a\}$, $\delta_{i,j}^0 = \delta_i^0(T_{i,j}) = \mathbf{1}\{\widetilde{W}_i(T_{i,j}) \in (a, b)\}$, and $\delta_{i,j}^b = \delta_i^b(T_{i,j}) = \mathbf{1}\{\widetilde{W}_i(T_{i,j}) \geq b\}$ represent whether an observation at $T_{i,j}$ is truncated from below, not truncated, or truncated from above, respectively. Consequently, the observed data are $\mathcal{D}_n = \left[\{W_i(\mathbf{T}_i), \mathbf{\Delta}_i(\mathbf{T}_i), \mathbf{X}_i, Y_i\} \right]_{i=1}^n$.

Prior to estimating the BLUPs for the FPC scores, the mean and covariance functions must be estimated. Often, non-parametric methods are used to smooth the sample mean and covariance estimators, however, using the same techniques on the truncated data introduces additional bias in the surface estimates. Our method centers on constructing estimators of $\mu(\cdot)$ and $\Sigma(\cdot, \cdot)$ that account for truncation through the maximization of the relevant local kernel-weighted log-likelihood functions. We obtain the FPC scores through a three-stage procedure: 1) construct estimators $\widehat{\mu}_n(t)$ of $\mu(t)$ and $\widehat{\sigma}_n^2(t)$ of $\tilde{\sigma}^2(t)$ over a pre-specified grid, 2) construct estimators $\widehat{\Sigma}_n(s, t)$ of $\widetilde{\Sigma}(s, t)$ and $\widehat{\Sigma}_n(s, t)$ of $\Sigma(s, t)$ over the same grid as in 1), 3) under the assumption that the random scores and latent noisy process $\widetilde{W}(\cdot)$ are jointly normal, formulate the FPC scores predictors.

Beginning with the first stage, let $A_h : \mathbb{R} \rightarrow \mathbb{R}$ denote a kernel function with bandwidth $h > 0$; in our applications we use a Gaussian kernel, but this is not essential. Define the observed-data local log-likelihood (Tibshirani and Hastie, 1987) at point $t \in [0, 1]$ as,

$$\begin{aligned} \ell_{n,h}\{t; \mu(t), \tilde{\sigma}^2(t)\} &= \sum_{i=1}^n \sum_{j=1}^{N_i} A_h(t - t_{i,j}) \left[\delta_{i,j}^a \log\left\{ \Phi\left(\frac{a - \mu(t)}{\tilde{\sigma}(t)}\right) \right\} \right. \\ &\quad \left. + \delta_{i,j}^0 \log\left\{ \phi\left(\frac{W_i(t_{i,j}) - \mu(t)}{\tilde{\sigma}(t)}\right) \right\} + \delta_{i,j}^b \log\left\{ 1 - \Phi\left(\frac{b - \mu(t)}{\tilde{\sigma}(t)}\right) \right\} \right]. \end{aligned}$$

Maximizing $\ell_{n,h}\{t; \mu(t), \tilde{\sigma}^2(t)\}$ at $t \in [0, 1]$ yields the local estimators $\hat{\mu}_n(t)$ and $\hat{\sigma}_n^2(t)$. The bandwidth is tuned using leave-one-curve-out cross-validation (CV) (Rice and Silverman, 1991). We note that the contributions to $\ell_{n,h}\{t; \mu(t), \tilde{\sigma}^2(t)\}$ from truncated points are non-positive, and potentially disproportionately smaller than contributions from non-truncated points in the same region. Simulation results suggest that in such cases, the CV procedure attempts to include more non-truncated points than what is optimal, thereby favoring larger bandwidths. We suggest that CV should be performed exclusively on the non-truncated observed points. The estimated optimal bandwidth is chosen to minimize the criterion function $CV_n(h) = \sum_{i=1}^n \sum_{j=1}^{N_i} \delta_{i,j}^0 \{W_i(t_{i,j}) - \hat{\mu}_n^{0,(-i)}(t, h)\}^2$, where $\hat{\mu}_n^{0,(-i)}(t, h)$ is the local mean estimate at time t under bandwidth h , computed from the data set excluding the i th trajectory and all truncated observations. Following bandwidth selection, local estimates of the mean function and variance-plus-measurement-error function are $\{\hat{\mu}_n(t), \hat{\sigma}_n^2(t)\} = \underset{\mu, \tilde{\sigma}^2}{\operatorname{argmax}} \ell_{n,h}\{t; \mu(t), \tilde{\sigma}^2(t)\}$. Measurement error variance and diagonal covariance elements are separated in the next step.

For the covariance surface estimation step, we begin by iteratively maximizing the local log-likelihood for each off-diagonal covariance element, under the constraint that each element update maintains the PSD structure of $\tilde{\Sigma}(\cdot, \cdot)$. Denote the set of upper triangular covariance matrix indices for unit i as $\mathcal{J}_i = \{(j, j') : j = 1, \dots, N_i, j' = 1, \dots, N_i, j < j'\}$. Let $B_{(h_1, h_2)} : \mathbb{R} \times \mathbb{R} \rightarrow \mathbb{R}$ denote a two-dimensional kernel function with bandwidths $h_1, h_2 > 0$. Because $\Sigma(\cdot, \cdot)$ is a symmetric operator, we choose $h = h_1 = h_2$; as a result, the notation $B_{(h_1, h_2)}$

simplifies to B_h . In our implementation we used a bivariate Gaussian kernel. The local log-likelihood for the off-diagonal element $\sigma(s, t)$ is,

$$\begin{aligned} & \ell_{n,h}\{s, t; \sigma(s, t), \mu(s), \mu(t), \tilde{\sigma}^2(s), \tilde{\sigma}^2(t)\} \\ &= \sum_{i=1}^n \sum_{(j,j') \in \mathcal{J}_i} B_h(s - t_{i,j}, t - t_{i,j'}) \\ & \times \left(\delta_{i,j}^0 \delta_{i,j'}^0 \log[p\{W_i(t_{i,j}), W_i(t_{i,j'})\}] \right) \end{aligned} \quad (2)$$

$$+ \delta_{i,j}^a \delta_{i,j'}^a \log[\Pr\{W_i(t_{i,j}) \leq a, W_i(t_{i,j'}) \leq a\}] \quad (3)$$

$$+ \delta_{i,j}^b \delta_{i,j'}^b \log[\Pr\{W_i(t_{i,j}) \geq b, W_i(t_{i,j'}) \geq b\}] \quad (4)$$

$$+ \delta_{i,j}^a \delta_{i,j'}^b \log[\Pr\{W_i(t_{i,j}) \leq a, W_i(t_{i,j'}) \geq b\}] \quad (5)$$

$$+ \delta_{i,j}^b \delta_{i,j'}^a \log[\Pr\{W_i(t_{i,j}) \geq b, W_i(t_{i,j'}) \leq a\}] \quad (6)$$

$$+ \delta_{i,j}^a \delta_{i,j'}^0 \log[\Pr\{W_i(t_{i,j}) \leq a \mid W_i(t_{i,j'}) \in (a, b)\} \times \phi\{\frac{W_i(t_{i,j'}) - \mu(t)}{\tilde{\sigma}(t)}\}] \quad (7)$$

$$+ \delta_{i,j}^b \delta_{i,j'}^0 \log[\Pr\{W_i(t_{i,j}) \geq b \mid W_i(t_{i,j'}) \in (a, b)\} \times \phi\{\frac{W_i(t_{i,j'}) - \mu(t)}{\tilde{\sigma}(t)}\}] \quad (8)$$

$$+ \delta_{i,j}^0 \delta_{i,j'}^a \log[\Pr\{W_i(t_{i,j'}) \leq a \mid W_i(t_{i,j}) \in (a, b)\} \times \phi\{\frac{W_i(t_{i,j}) - \mu(s)}{\tilde{\sigma}(s)}\}] \quad (9)$$

$$+ \delta_{i,j}^0 \delta_{i,j'}^b \log[\Pr\{W_i(t_{i,j'}) \geq b \mid W_i(t_{i,j}) \in (a, b)\} \times \phi\{\frac{W_i(t_{i,j}) - \mu(s)}{\tilde{\sigma}(s)}\}]], \quad (10)$$

where (2) is the bivariate Gaussian density with mean $\boldsymbol{\mu}_{s,t} = \{\mu(s), \mu(t)\}^\top$ and covariance matrix $\boldsymbol{\Psi}_{s,t}$, which is composed of off-diagonal element $\sigma(s, t)$ and variance elements $\tilde{\sigma}^2(s)$ and $\tilde{\sigma}^2(t)$; (3) – (6) are probabilities from the corresponding cdf; conditional probabilities in (7) – (10) rely on conditional mean and variance parameters that follow from results on a partitioned multivariate Gaussian vectors (see the Supplemental Materials for further details).

The off-diagonal elements of both $\widehat{\Sigma}_n(\cdot, \cdot)$ and $\widetilde{\Sigma}_n(\cdot, \cdot)$, are populated with $\widehat{\sigma}_n(s, t) = \operatorname{argmax}_{\sigma(s,t)} \ell_{n,h}\{s, t; \sigma(s, t), \widehat{\mu}_n(s), \widehat{\mu}_n(t), \widehat{\sigma}_n^2(s), \widehat{\sigma}_n^2(t)\}$. Estimators of $\boldsymbol{\mu}_{s,t}$ and $\{\tilde{\sigma}^2(s), \tilde{\sigma}^2(t)\}$ are available from the previous stage. Projected gradient descent is used to maintain the PSD structure of $\widetilde{\Sigma}(\cdot, \cdot)$ during optimization. Let $\widetilde{\Sigma}_n(\cdot, \cdot)$ denote the matrix with (s, t) th element $\widehat{\sigma}_n(s, t) \mathbb{1}_{s \neq t} + \widehat{\sigma}_n^2(s) \mathbb{1}_{s=t}$. For notational convenience, define the set of timestamps for non-

truncated recordings from the i th trajectory by $\mathbf{T}_i^0 = \{T_{i,j} : \delta_{i,j}^0 = 1\}$. The corresponding vector of non-truncated measurements is $W_i(\mathbf{T}_i^0)$, and the matrix $\widehat{\Sigma}_n(\mathbf{T}_i^0, \mathbf{T}_i^0)$ has the analogous rows and columns of $\widehat{\Sigma}_n(\cdot, \cdot)$. While leave-one-curve-out CV may be used to select the bandwidth, a less computationally intensive option is to select the bandwidth h (or the bandwidth pair (h_s, h_t)) that maximizes the pseudo-likelihood $\widehat{\mathcal{L}} = \prod_{i=1}^n p_0\{W_i(\mathbf{t}_i^0)\}$, where p_0 denotes the Gaussian density with mean $\widehat{\mu}_n(\mathbf{T}_i^0)$ and covariance $\widehat{\Sigma}_n(\mathbf{T}_i^0, \mathbf{T}_i^0)$ for the non-truncated data from unit i .

Assuming the measurement errors and stochastic realizations are independent, a smooth estimator of $\Sigma(\cdot, \cdot)$ can be obtained by removing the diagonal elements of $\widehat{\Sigma}_n(\cdot, \cdot)$, then applying a two-dimensional local smoother to estimate the diagonal elements of $\Sigma(\cdot, \cdot)$. We follow Yao et al.'s (2003) suggestion to use a local quadratic term for the direction perpendicular to the diagonal, and local linear term for the direction parallel to the diagonal. Define the local smoother $D_{n,h}\{s, t; \boldsymbol{\beta}, \widehat{\Sigma}_n(\mathbf{T}, \mathbf{T})\} = \sum_{i=1}^n \sum_{1 \leq j \neq j' \leq N_i} B_h(s - T_{i,j}, t - T_{i,j'}) [\widehat{\Sigma}_n(T_{i,j}^*, T_{i,j'}^*) - \{\beta_0 + \beta_1(s - T_{i,j}^*) + \beta_2(t - T_{i,j'}^*)^2\}]$, where $B_h(\cdot, \cdot)$ is a two-dimensional Gaussian kernel, and the time index pair $(T_{i,j}^*, T_{i,j'}^*)$ represents the $\pi/4$ radian rotation of $(T_{i,j}, T_{i,j'})$ to the right (Yao et al., 2003). The rotation of the axes permits the direct use of h from the $\widehat{\sigma}^2(t)$ optimization step, negating the formulation of an additional bandwidth selection criterion. However, the use of $D_{n,h}$ does not guarantee a resulting PSD matrix, so we enforce the additional constraints that 1) $\widehat{\beta}_{n,0}(t) \leq \widehat{\sigma}_n^2(t)$ and 2) the SVD of $\widehat{\Sigma}_n(\mathbf{T}, \mathbf{T})$ yields non-negative eigenvalues. Under these constraints, the smoothed diagonal estimators of the covariance operator are $\widehat{\Sigma}_n(t, t) = \widehat{\beta}_{n,0}(t)$, from $\operatorname{argmin}_{\boldsymbol{\beta}} D_{n,h}\{s, t; \boldsymbol{\beta}, \widehat{\Sigma}_n(\mathbf{T}, \mathbf{T})\}$. Consequently, the measurement error variance estimator is given by $\widehat{\sigma}_n^2(t) = \widehat{\Sigma}_n(t, t) - \widehat{\Sigma}_n(t, t)$. Eigenvalue and eigenvectors of the form $\{\lambda_k, \phi_k(\mathbf{T})\}$ may be estimated for $1 \leq k \leq N$ from the SVD of the $N \times N$ matrix $\widehat{\Sigma}_n(\mathbf{T}, \mathbf{T})$. Further details regarding the algorithm used for the covariance optimization are provided in the appendix.

To construct the random score predictors for the third stage, we adapt the conditional expectation approach (Yao et al., 2005). Recall that the non-truncated data and FPC scores are jointly normal, so we may first consider treating the truncated points as missing entirely. The BLUP of the k th FPC for unit i follows immediately: $\tilde{\xi}_{i,k}^0 = \mathbb{E}\{\xi_{i,k} \mid W_i(\mathbf{T}_i^0) = w_i(\mathbf{t}_i^0)\} = \lambda_k \phi_k(\mathbf{t}_i^0)^\top \tilde{\Sigma}(\mathbf{t}_i^0, \mathbf{t}_i^0)^{-1} \{w_i(\mathbf{t}_i^0) - \mu(\mathbf{t}_i^0)\}$. Potentially, much of the data are removed if trajectories have large truncated regions. To avoid a large discard of data, we construct a BLUP, conditional on all of the observed trajectory data and truncation indicators: $\xi_{i,k}^* := \mathbb{E}\{\xi_{i,k} \mid W_i(\mathbf{T}_i) = w_i(\mathbf{t}_i), \Delta_i(\mathbf{T}_i) = \delta_i(\mathbf{t}_i)\}$. The predictor can be rewritten as,

$$\begin{aligned} \xi_{i,k}^* &= \mathbb{E}\{\xi_{i,k} \mid W_i(\mathbf{T}_i) = w_i(\mathbf{t}_i), \Delta_i(\mathbf{T}_i) = \delta_i(\mathbf{t}_i)\} \\ &= \mathbb{E}[\mathbb{E}\{\xi_{i,k} \mid \widetilde{W}_i(\mathbf{T}_i) = \widetilde{w}_i(\mathbf{t}_i)\} \mid W_i(\mathbf{T}_i) = w_i(\mathbf{t}_i), \Delta_i(\mathbf{T}_i) = \delta_i(\mathbf{t}_i)] \quad (11) \\ &= \mathbb{E}\{\widetilde{\xi}_{i,k} \mid W_i(\mathbf{T}_i) = w_i(\mathbf{t}_i), \Delta_i(\mathbf{T}_i) = \delta_i(\mathbf{t}_i)\}, \end{aligned}$$

where (11) follows from the assumption (A5) $Z_i(\cdot) \perp \{W_i(\cdot), \Delta_i(\cdot)\} \mid \widetilde{W}_i(\cdot)$, and $\widetilde{\xi}_{i,k}$ is the BLUP described in Section 2. However, $\widetilde{\xi}_{i,k}$ is not directly estimable because $\widetilde{W}_i(\mathbf{T}_i)$ is not fully observed in truncated regions. Therefore, we approximate $\xi_{i,k}^*$ with the estimator $\widehat{\xi}_{n,i,k}$, which is computed by sampling m vectors, $\widetilde{W}_i(\mathbf{T}_i) \mid W_i(\mathbf{T}_i) = w_i(\mathbf{t}_i), \Delta_i(\mathbf{T}_i) = \delta_i(\mathbf{t}_i)$, then plugging each vector into $\widehat{\xi}_{n,i,k}$ from Section 2 and taking the average over the m estimates.

Sampling the latent noisy discretized process, conditional on the observed data and truncation indicators, is equivalent to sampling the truncated regions, conditional on the non-truncated data and truncation indicators, and updating $\widetilde{W}_i(\mathbf{t}_i)$ accordingly. To do so, reorder \mathbf{t}_i for each unit i such that the non-truncated data indices are first and the truncated data indices are grouped together after; this reordered time index set is denoted by $\widetilde{\mathbf{t}}_i$. The partially observed noisy process for unit i on the observed grid $\widetilde{\mathbf{t}}_i$ may be partitioned as follows: $\widetilde{W}_i(\widetilde{\mathbf{t}}_i) = \{\widetilde{W}_i(\widetilde{\mathbf{t}}_i^0), \widetilde{W}_i(\widetilde{\mathbf{t}}_i \setminus \widetilde{\mathbf{t}}_i^0)\}^\top := \{\widetilde{\mathbf{W}}_{i,1}, \widetilde{\mathbf{W}}_{i,2}\}^\top$ with $\widetilde{W}(\widetilde{\mathbf{t}}_i) \sim \mathcal{N}\{\mu(\widetilde{\mathbf{t}}_i), \widetilde{\Sigma}(\widetilde{\mathbf{t}}_i, \widetilde{\mathbf{t}}_i)\}$. Previously estimated mean and covariance parameters are plugged in for $\mu(\widetilde{\mathbf{t}}_i)$ and $\widetilde{\Sigma}(\widetilde{\mathbf{t}}_i, \widetilde{\mathbf{t}}_i)$. Results on partitioned multivariate Gaussian vectors are utilized to

sample m , $|\mathbf{T}_i \setminus \mathbf{T}_i^0|$ -dimensional vectors from $\widetilde{\mathbf{W}}_{i,2} \mid W_i(\mathbf{T}_i) = w_i(\mathbf{t}_i), \Delta(\mathbf{T}_i) = \delta(\mathbf{t}_i) \sim$ Truncated Normal($\boldsymbol{\mu}_{\widetilde{\mathbf{W}}_{i,2}|\widetilde{\mathbf{W}}_{i,1}}, \boldsymbol{\Sigma}_{\widetilde{\mathbf{W}}_{i,2}|\widetilde{\mathbf{W}}_{i,1}}, \mathbf{a}^*, \mathbf{b}^*$), where \mathbf{a}^* has elements set to b when $\delta_i^b(t) = 1$ (i.e., $\mathbb{1}\{\widetilde{w}_{2,i} \geq b\} = 1$) and $-\infty$ when $\delta_i^b(t) = 0$ (not truncated or truncated at the lower bound) and \mathbf{b}^* has elements set to a when $\delta_i^a(t) = 1$ (i.e., $\mathbb{1}\{\widetilde{w}_{2,i} \leq a\} = 1$) and ∞ when $\delta_i^a(t) = 0$ (not truncated or truncated at the upper bound). Subsequent samples are populated in the relevant entries of $\widetilde{W}_i(\mathbf{t}_i)$, then the m $\widehat{\xi}_{n,i,k}$'s are computed and averaged together, yielding $\widehat{\xi}_{n,i,k}$. Under the assumption that the i th functional process may be well-approximated by the first K FPC scores, the predicted trajectory unit i is $\widehat{W}_{n,i}^K(t) = \widehat{\mu}_n(t) + \sum_{k=1}^K \widehat{\xi}_{n,i,k} \widehat{\phi}_{n,k}(t)$.

Now, we illustrate the use of $\widehat{\xi}_{n,i,k}$ in the GFLM,

$$\begin{aligned} & g[\mathbb{E}\{Y_i \mid \mathbf{X}_i = \mathbf{x}_i, W_i(\mathbf{T}_i) = w_i(\mathbf{t}_i), \Delta_i(\mathbf{T}_i) = \delta_i(\mathbf{t}_i)\}] \\ &= g\left(\mathbb{E}\left[\mathbb{E}\{g^{-1}(\alpha_0^* + \mathbf{x}_i^\top \boldsymbol{\alpha} + \sum_{k \geq 1} \beta_k \xi_{i,k}) \mid \mathbf{X}_i = \mathbf{x}_i, \widetilde{W}_i(\mathbf{T}_i) = \widetilde{w}_i(\mathbf{t}_i)\} \mid \right. \right. \\ & \quad \left. \left. \mathbf{X}_i = \mathbf{x}_i, W_i(\mathbf{T}_i) = w_i(\mathbf{t}_i), \Delta_i(\mathbf{T}_i) = \delta_i(\mathbf{t}_i)\right]\right), \end{aligned} \quad (12)$$

where the equality follows from assumptions (A5), (A6) $Y_i \perp \{W_i(\cdot), \Delta_i(\cdot)\} \mid \{Z_i(\cdot), \mathbf{X}_i\}$, (A7) $Y_i \perp \{W_i(\cdot), \Delta_i(\cdot)\} \mid \{\widetilde{W}_i(\cdot), \mathbf{X}_i\}$, and (A2). We assume the regression is reasonably approximated by the first K FPC scores, where K is selected by the FVE. The coefficients $(\alpha_0^*, \boldsymbol{\alpha}^\top, \beta_1, \dots, \beta_K)$ may be estimated via maximum likelihood.

We establish convergence rates for the GFLM when $Y_i \in \mathbb{R}$ and $g(\cdot)$ is the identity link. Let $M\{\mathbf{x}, w(\mathbf{t}), \delta(\mathbf{t})\} := \mathbb{E}\{Y \mid \mathbf{X} = \mathbf{x}, W(\mathbf{T}) = w(\mathbf{t}), \Delta(\mathbf{T}) = \delta(\mathbf{t})\}$. In addition to (A1) - (A7), the following assumptions are used: (A8) $\lim_{n \rightarrow \infty} \bigcup_{i=1}^n \mathbf{T}_i$ forms a dense set in $[0, 1]$ with probability 1; (A9) $\sup_t |\widehat{\mu}_n(t) - \mu(t)| = O_p(n^{-\zeta_\mu})$ for $t \in [0, 1]$ and some positive ζ ; (A10) $\sup_{s,t} |\widehat{\Sigma}_n(s,t) - \Sigma(s,t)| = O_p(n^{-\zeta_\Sigma})$ for $s, t \in [0, 1]$ and some positive ζ ; (A11) $\sup_t |\widehat{\sigma}_n^2(t) - \sigma^2(t)| = O_p(n^{-\zeta_\sigma})$ for $t \in [0, 1]$ and some positive ζ ; (A12) $\mathbb{E}\|\mathbf{X}\|^4$ and $\mathbb{E}(\mathbf{X}\mathbf{X}^\top)$ is nonsingular; and (A13) $|\beta_k| \leq Ck^{-\eta}$ for all $k \geq 1$, and some $\eta > 1$ and $C > 0$.

THEOREM 1: *Let K_n be an increasing sequence of integers such that $K_n \rightarrow \infty$ and $K_n/n^{2\zeta} \rightarrow 0$ as $n \rightarrow \infty$. Under assumptions (A1) - (A13),*

$$\mathbb{E} \left[\left\| \widehat{M}_n^{K_n} \{ \mathbf{X}, W(\mathbf{T}), \boldsymbol{\Delta}(\mathbf{T}); \widehat{\boldsymbol{\theta}}_n^{K_n} \} - M \{ \mathbf{X}, W(\mathbf{T}), \boldsymbol{\Delta}(\mathbf{T}) \} \middle| \mathcal{D}_n \right\| \right] = O_p(K_n n^{-1/2} + K_n^{1/2} n^{-\zeta}),$$

where $\zeta = \min(\zeta_\mu, \zeta_\Sigma, \zeta_\sigma)$ and $\widehat{\boldsymbol{\theta}}^{K_n} = (\widehat{\boldsymbol{\alpha}}_{n,0}^*, \widehat{\boldsymbol{\alpha}}_n^\top, \widehat{\boldsymbol{\beta}}_{n,1}, \dots, \widehat{\boldsymbol{\beta}}_{n,K_n})^\top$.

The proof is provided in the Supplemental Material.

4. Simulation Study

We evaluate the finite sample performance of the proposed estimator in a suite of simulation experiments. As a baseline, we also implemented the proposed estimation procedure under the incorrect assumption that the data are free from truncation (termed the naïve method) and the canonical PACE method (Yao et al., 2005) which also does not account for truncation. Performance is measured in terms of the SSE for the mean, covariance, measurement error variance, and signal-to-noise ratio (SNR) estimators; for the regression settings, either the MSE or classification accuracy is used, depending on the model. For all simulations: $t \in [0, 1]$, the true mean function is $\mu(t) = \sin(2\pi t)$, and the measurement error is chosen so that the signal-to-noise ratio (SNR) resembles that from the CGM device discussed in Section 5 (Nagl et al., 2020). The observation interval is discretized to a grid of $g = 15$ equally spaced points, $\mathbf{t} = \{t_1, \dots, t_g\}$, and for each unit, the number of observations is sampled from $N_i \sim \text{Uniform}\{5, \dots, g\}$, then timestamps are sequentially sampled from $T^{(1)} \mid N_i = n_i \sim \text{Uniform}\{\mathbf{t}\}$ and $T^{(j+1)} \mid N_i = n_i, T^{(1)} = t^{(1)}, \dots, T^{(j)} = t^{(j)} \sim \text{Uniform}[\mathbf{t} \setminus \{\bigcup_{k=1}^j t^{(k)}\}]$. The subsequent ordered observation times for unit i are $\mathbf{T}_i = \{\bigcup_{j=1}^{N_i} t^{(j)}\}$. Discretized measurements from $n = 100$ trajectories are generated from the model $\mathbf{W}_i \mid N_i = n_i, \mathbf{T}_i = \mathbf{t}_i, \overset{\text{iid}}{\sim} \mathcal{N}\{\mu(\mathbf{t}_i), \widetilde{\Sigma}(\mathbf{t}_i, \mathbf{t}_i)\}$, then truncated so that all $w_i(t_{i,j}) \in [-1, 1]$.

Five simulation settings are considered. The choices of covariance operator and measurement error variance differentiate the cases. The first four cases illustrate the performance

of the mean and covariance estimation procedures as the covariance structure builds in complexity. The fifth case demonstrates the recovery of principal components, as well as the use of FPC score estimates for the GFLM.

(Case 1) $\Sigma(\mathbf{T}, \mathbf{T}) = 0.5\mathbf{I}$ and $\sigma^2(\mathbf{T}) = 0.05$.

(Case 2) $\Sigma(\mathbf{T}, \mathbf{T})$ has an AR(1) correlation structure with correlation parameter $\rho = 0.9$ and variance parameter $\psi = 0.5$. Again, $\sigma^2(\mathbf{T}) = 0.05$.

(Case 3) $\Sigma(\mathbf{T}, \mathbf{T})$ has a block diagonal structure. An AR(1) structure is enforced for all diagonal $g/3 \times g/3$ -dimensional blocks with variance $\psi = 0.5$. Let $\rho_1 = 0.5$ for the upper left block, $\rho_2 = 0.7$ for the middle, and $\rho = 0.9$ for the bottom right. The measurement error variance is 0.05.

(Case 4) $\Sigma(\mathbf{T}, \mathbf{T})$ has the same structure as in Case 2, except the measurement error is doubled in regions where $\mu(\cdot) < -0.5$ and halved in regions where $\mu(\cdot) > 0.5$ to resemble the estimated measurement error from the device used in our application (Nagl et al. 2020).

(Case 5) We construct $\Sigma(\mathbf{T}, \mathbf{T})$ from eigenfunctions $\phi_1(t) = -\sqrt{2}\cos(\pi t)$, $\phi_2(t) = -\sqrt{2}\sin(\pi t)$, and $\{\phi_k(t)\}_{k=3}^g$ (for $k \geq 3$, the of randomly generated and orthogonalized using QR factorization). Corresponding eigenvalues are of the form $\lambda_k = \frac{1}{14k^2}$ and $\sigma^2(\mathbf{T}) = 0.05$.

On average, one third of the measurements are truncated for settings 1 - 4 and 20% are truncated for the fifth case. For the regression setting, we generate the underlying process $\mathbf{Z}_i \mid N_i = n_i, \mathbf{T}_i = \mathbf{t}_i, \overset{iid}{\sim} \mathcal{N}\{\mu(\mathbf{t}_i), \Sigma(\mathbf{t}_i, \mathbf{t}_i)\}$ and choose $\beta(t) = 1$. Two GFLM settings are considered: the continuous response $Y_i = \sum_{k \geq 1} \beta_k \xi_{i,k} + \omega_i$ with $\omega_i \overset{iid}{\sim} \mathcal{N}(0, 1)$ and the identity link function, and the binary response, $Y_i = \mathbb{1}\{\sum_{k \geq 1} \beta_k \xi_{i,k} > 0\}$, with the logit link function.

Table 1 shows the SSE for the mean and covariance estimators, averaged over 100 MC samples, for all three estimation procedures. The proposed mean estimator performs best for all cases and the covariance estimator performs best for settings 2 - 5. Table 2 shows the average MC SSE for the measurement error variance estimator and the signal-to-noise ratios

(SNRs) which are defined by $\text{SNR} := \hat{\sigma}^2(t)/\tilde{\sigma}^2(t)$ at time t . The measurement error variance SSE is larger for $\hat{\sigma}^2(\cdot)$ than for either $\hat{\sigma}^{2,N}(\cdot)$ or $\hat{\sigma}^{2,\text{CE}}(\cdot)$, however this can be explained by the SNRs. *Cases 2 - 5* show favorable results for our proposed method based on the SNR, however both the naïve and PACE procedures underestimate the diagonal of $\tilde{\Sigma}(\cdot, \cdot)$, leading to a smaller measurement error variance estimate, but inaccurate SNR.

[Table 1 about here.]

[Table 2 about here.]

Additionally, our method demonstrates better recovery of dominant eigenfunctions than the comparable procedures. The first eigenfunction from *Case 5* is shown in Figure 1, overlaid with the respective estimates from all three cases.

[Figure 1 about here.]

Applications to the GFLM show robustness to biased mean and covariance surface estimates. The continuous response regression resulted in an MSE of 0.89 for the proposed procedure, 0.89 for the naïve version, and 0.96 for the PACE settings (averaged over 100 MC samples). The logistic GFLM model yielded an average classification accuracy of 80.44% under our proposed procedure, 82.51% under the naïve counterpart, and 79.51% under the canonical PACE method.

5. Application: Eating Disorder Classification

Individuals with type 1 diabetes (T1D) and poor glycemic control exhibit blood glucose readings that are both more variable and higher on average than those of individuals with T1D and better glycemic control. These concerns are typically exaggerated if the patient with T1D has an eating disorder (ED) diagnosis or symptomatology. Insufficient insulin dosing prevents the utilization of glucose for energy and promotes the breakdown of fat as

an alternative energy source; consequently, insulin omission alone, or following an overeating episode, is a sign of disordered behavior in patients with T1D that results in elevated post-prandial blood glucose levels for an abnormally long period of time. Coupled with appropriate diagnostic instruments, glucose trajectory characteristics may be used to distinguish between individuals with and without EDs. Continuous glucose monitors (CGMs) estimate blood glucose levels from interstitial fluids, providing a trajectory of glucose recordings across a discretized grid of times, which can be used to inform diabetes management decisions. However, the accompanying CGM software truncates readings to “High” if the recording is ≥ 400 mg/dL and “Low” if it is ≤ 40 mg/dL (from a clinical perspective, truncation is reasonable because all values outside of the range are dangerous to the patient). Therefore, instead of observing an individual’s true blood glucose trajectory, we record noisy, and possibly truncated, readings in five minute increments.

We analyze the following subset of data from the Eating Disorders in Type 1 Diabetes: Mechanisms of Comorbidity clinical study (R01 DK089329, PI: Merwin): 75 minutes of post-meal CGM recordings, baseline characteristics, and ED status for $n = 59$ patients (45 of whom have diagnosed EDs or ED symptomatology). Data for each study participant are of a form similar to that discussed in Section 3. Observation times represent the time difference between a CGM recording and the start of the meal, and are re-scaled so that all differences fall in the interval $[0, 1]$. Baseline covariates include HbA1C, number of years since T1D diagnosis, and age. The outcome of interest is the ED indicator (1 if patient i has an ED diagnosis or symptomatology, and 0 otherwise). Figure 2 shows the glucose recordings from a training set with the smoothed mean estimate overlaid in red (left), as well as the covariance surface estimate (right). On average, glucose levels begin to spike almost immediately post meal, then level off after one hour and as expected, the T1D patients without EDs run lower

on average than their ED counterparts. We train the binary response GFLM using 5-fold CV, and the average accuracy across test sets is 0.867.

[Figure 2 about here.]

6. Discussion

We presented a procedure to estimate FPC scores, centered around the accurate recovery of smoothed mean and covariance functions, that is appropriate for truncated and non-truncated data, with or without measurement error. The incorporation of neighboring points during the mean and covariance stages allows local estimation in sparsely observed areas to borrow information from neighboring regions, making the method feasible for both densely and sparsely observed data. Optimization and smoothing are done concurrently, thereby removing the need to retroactively smooth surface estimates, and the smoothed covariance surface maintains a PSD structure, unlike standard two-dimensional smoothers. FPC score predictors are estimated by exploiting the joint normality of the random scores and the noisy process $\widetilde{W}(\cdot)$. Lastly, we demonstrated how the FPC scores can be utilized for scalar-on-function regression.

While irregularly spaced and sparsely observed data were considered, extensions to 1) data requiring trajectory alignment and 2) settings for which units have repeated functional measurements, so-called second-generation functional data (Koner and Staicu, 2023), were not addressed. The former is particularly relevant if there are external events that may alter the functional process at any period in the observation window. If event times are random, the resulting trajectories may be misaligned in time. A variety of time warping techniques have been proposed to address this issue for the non-truncated case (Wang et al., 2016). Extensions of this methodology to the truncated data case are particularly relevant

to longer trajectory data, such as daily blood glucose recordings for which meal times are not aligned.

REFERENCES

- Besse P, and Ramsay JO. (1986). Principal components analysis of sampled functions. *Psychometrika*, 51(2), 285–311.
- Dauxois, J., Pousse, A. and Romain, Y. (1982). Asymptotic theory for the principal component analysis of a vector random function: some applications to statistical inference. *Journal of Multivariate Analysis* 12, 136–154.
- Hall, P., and Hooker, G. (2016). Truncated linear models for functional data. *Journal of the Royal Statistical Society Series B: Statistical Methodology*, 78(3), 637-653.
- Higham, N. (2002). Computing the nearest correlation matrix - a problem from finance. *IMA Journal of Numerical Analysis*, 22, 329–343.
- James, G. (2002). Generalized linear models with functional predictors. *Journal of the Royal Statistical Society. Series B (Statistical Methodology)*, 64(3), 411–432.
- James, G., Hastie, T., and Sugar, C. (2000). Principal component models for sparse functional data. *Biometrika* 87(3), 587-602.
- Karhunen, K. (1946). Zur spektraltheorie stochastischer prozesse. *Issue 34 of Annales Academiae scientiarum Fennicae*, 37.
- Koner, S., and Staicu, A.-M. (2023). Second-generation Functional Data. *Annual Review of Statistics and Its Application*, 10(1), 547–572.
- Laber, E. B., and Staicu, A.-M. (2018). Functional feature construction for individualized treatment regimes. *Journal of the American Statistical Association*, 113(523), 1219–1227.
- Liu, X., Divani, A., and Petersen, A. (2022). Truncated estimation in functional generalized linear regression models. *Computational Statistics and Data Analysis*, 169(C).

- Loève, M. (1946). Fonctions aléatoires à décomposition orthogonale exponentielle. *La Revue Scientifique*, 84, 159–162.
- Marx, B., and Eilers, P. (1999). Generalized linear regression on sampled signals and curves: a P-spline approach. *Technometrics* 41(1), 1–13.
- Morris, J. (2015). Functional regression. *Annual Review of Statistics and Its Application*, 2, 321-359.
- Morris, S., and Carroll, J. (2006). Wavelet-based functional mixed models. *Journal of the Royal Statistical Society: Series B (Statistical Methodology)*, 68(2), 179-199.
- Müller, H.G., and Stadtmüller, U. (2005). Generalized functional linear models. *The Annals of Statistic*, 33(2), 774–805.
- Nagl, K., Berger, G., Aberer, F., Ziko, H., Weimann, K., Bozic, I., Rami-Merhar, B., and Mader, J. K. (2020). Performance of three different continuous glucose monitoring systems in children with type 1 diabetes during a diabetes summer camp. *Pediatric Diabetes*, 22(2), 271–278.
- Ramsay, J., and Dalzell, C. (1991). Some tools for functional data analysis. *Journal of the Royal Statistical Society. Series B (Methodological)*, 53(3), 539-561.
- Ramsay, J. O., and Silverman, B. W. (2005). *Functional Data Analysis (2nd ed.)*. Springer.
- Rice, J., Silverman, B., (1991). Estimating the Mean and Covariance Structure Nonparametrically When the Data are Curves. *Journal of the Royal Statistical Society. Series B (Methodological)*, 53(1), 233-243.
- Rigobon, R., and Stoker, T. M. (2009). Bias from censored regressors. *Journal of Business and Economic Statistics*, 27(3), 340-353.
- Rigobon, R., and Stoker, T. M. (2007). Estimation with Censored Regressors: Basic Issues. *International Economic Review*, 48(4), 1441–146.
- Staicu, A.-M, Li, Y., Crainiceanu, C. M., and Ruppert, D. (2014). Likelihood ratio tests

for dependent data with applications to longitudinal and functional data analysis. *Scandinavian Journal of Statistics*, 41(4), 932–949.

Tibshirani, R., and Hastie, T. (1987). Local Likelihood Estimation. *Journal of the American Statistical Association*, 82(398), 559–567.

Yao, F., Müller, H. G., Clifford, A. J., Dueker, S. R., Follett, J., Lin, Y., Buchholz, B. A., and Vogel, J. S. (2003). Shrinkage estimation for functional principal component scores with application to the population kinetics of plasma folate. *Biometrics*, 59(3), 676–685.

Yao, F., Müller, H. G., and Wang, J. L. (2005). Functional data analysis for sparse longitudinal data. *Journal of the American Statistical Association*, 100(470), 577–590.

Wang, J.-L., Chiou, J.-M., and Müller, H.-G. (2016). Functional data analysis. *Annual Review of Statistics and Its Application*, 3(1), 257–295.

APPENDIX

Partitioned Multivariate Gaussian Vectors

For the covariance optimization procedure and the FPC score MC estimates, we utilize the following results on partitioned multivariate Gaussian vectors.

For $\begin{pmatrix} \mathbf{X}_1 \\ \mathbf{X}_2 \end{pmatrix} \sim \mathcal{N}_{p_1+p_2}(\boldsymbol{\mu}, \boldsymbol{\Sigma})$ where $\boldsymbol{\mu} = \begin{pmatrix} \boldsymbol{\mu}_1 \\ \boldsymbol{\mu}_2 \end{pmatrix}$ and $\boldsymbol{\Sigma} = \begin{pmatrix} \boldsymbol{\Sigma}_{11} & \boldsymbol{\Sigma}_{12} \\ \boldsymbol{\Sigma}_{21} & \boldsymbol{\Sigma}_{22} \end{pmatrix}$,

- (1) $\mathbf{X}_1 \sim \mathcal{N}_{p_1}(\boldsymbol{\mu}_1, \boldsymbol{\Sigma}_{11})$;
- (2) $\mathbf{X}_2 \sim \mathcal{N}_{p_2}(\boldsymbol{\mu}_2, \boldsymbol{\Sigma}_{22})$;
- (3) $\mathbf{X}_1 \mid \mathbf{X}_2 = \mathbf{x}_2 \sim \mathcal{N}_{p_1}\{\boldsymbol{\mu}_1 + \boldsymbol{\Sigma}_{12}\boldsymbol{\Sigma}_{22}^{-1}(\mathbf{x}_2 - \boldsymbol{\mu}_2), \boldsymbol{\Sigma}_{11} - \boldsymbol{\Sigma}_{12}\boldsymbol{\Sigma}_{22}^{-1}\boldsymbol{\Sigma}_{21}\}$;
- (4) $\mathbf{X}_2 \mid \mathbf{X}_1 = \mathbf{x}_1 \sim \mathcal{N}_{p_2}\{\boldsymbol{\mu}_2 + \boldsymbol{\Sigma}_{21}\boldsymbol{\Sigma}_{11}^{-1}(\mathbf{x}_1 - \boldsymbol{\mu}_1), \boldsymbol{\Sigma}_{22} - \boldsymbol{\Sigma}_{21}\boldsymbol{\Sigma}_{11}^{-1}\boldsymbol{\Sigma}_{12}\}$.

Covariance Optimization

Projected stochastic gradient descent is performed for each off-diagonal element of the matrix $\tilde{\boldsymbol{\Sigma}}$. Let $\mathbf{W} \in \mathbb{R}^{n \times |\mathbf{T}|}$ denote the matrix of all observed trajectory data, where the

i th row contains the functional data for unit i . Columns reference the timestamps $\mathbf{T} = \bigcup_{i=1}^n \mathbf{T}_i$, so \mathbf{W} will contain missing entries if units are observed on different grids, or if they have true missing data. Projected stochastic gradient descent is performed for each off-diagonal element of the matrix $\tilde{\Sigma}$ to maintain the PSD structure. The gradient update $\nabla_{\sigma_{j,j'}} \{\ell^{(t_j, t_{j'})}, h(\sigma_{j,j'}^{(r-1)}; \hat{\mu}_{j,j'}(\mathbf{t}), \hat{\Sigma}_j^2(\mathbf{t}), \hat{\Sigma}_{j'}^2(\mathbf{t}))\}$ is the derivative of the local log-likelihood with respect to $\sigma_{j,j'}$ at $\sigma_{j,j'}^{(r-1)}$. Additionally, we offer the following ad hoc approach to step size updates that performed better (in terms of the number of iterations required until tolerance requirements were met) than both AdaGrad and constant step size. For one iteration over all parameters, if the average $\alpha^{(r)}$ is close to one, that implies each parameter was able to take a full (or almost full) gradient step, even under the PSD requirement. If the average $\alpha^{(r)}$ is near 0, that indicates the step size is too large. Therefore, if the average $\alpha^{(r)}$ is $= 1$ (< 0.5), we increase (decrease) the step size for the next iteration, $\epsilon^{(r+1)}$, by 10%. To avoid oscillatory update behavior for the last few parameters, we suggest decreasing the step size by 50% if $\text{sign}(\sigma_{j,j'}^{(r-3)} - \sigma_{j,j'}^{(r-2)}) = \text{sign}(\sigma_{j,j'}^{(r)} - \sigma_{j,j'}^{(r-1)}) \neq \text{sign}(\sigma_{j,j'}^{(r-2)} - \sigma_{j,j'}^{(r-1)})$ and $|\sigma_{j,j'}^{(r-2)} - \sigma_{j,j'}^{(r-3)}| < |\sigma_{j,j'}^{(r)} - \sigma_{j,j'}^{(r-1)}|$ (collectively referred to as ‘criterion 1’). The algorithm runs as follows.

Algorithm 1 $\widetilde{\Sigma}(\cdot, \cdot)$ optimization procedure for bandwidth h

Input: $\{w_i(\mathbf{t}_i), \boldsymbol{\delta}_i(\mathbf{t}_i), \widehat{\boldsymbol{\mu}}(\mathbf{T}_i), \widehat{\boldsymbol{\Sigma}}^2(\mathbf{t}_i)\}_{i=1}^n$

1: **Initialize:** $\widetilde{\Sigma}^{(0)} = \text{Cov}\{w(\mathbf{t}_i)\}$, $\text{diag}(\widetilde{\Sigma}^{(0)}) = \widehat{\boldsymbol{\sigma}}^2(\mathbf{t}_i)$, initial step-size $\epsilon^{(1)}$, upper triangle indices \mathcal{J} , tolerance τ

2: **if** $\widetilde{\Sigma}^{(0)}$ is not PSD **then** $\widetilde{\Sigma}^{(0)} =$ nearest PSD $\widetilde{\Sigma}^{(0)}$ (maintaining the diagonal) (Higham, 2002)

3: **while** $|\widetilde{\Sigma}_{j,j'}^{(r)} - \widetilde{\Sigma}_{j,j'}^{(r-1)}| > \tau$ for any $(j, j') \in \mathcal{J}$ **do**

4: Shuffle \mathcal{J}

5: $\widetilde{\Sigma}_{j,j'}^{(r)} = \widetilde{\Sigma}_{j,j'}^{(r-1)}$

6: **for** $(j, j') \in \mathcal{J}$ **do**

7: $\sigma_{j,j'}^{*(r)} = \sigma_{j,j'}^{(r-1)} + \epsilon^{(r)} \nabla_{\sigma_{j,j'}} \{\ell^{(t_j, t_{j'})}, h(\sigma_{j,j'}^{(r-1)}; \widehat{\boldsymbol{\mu}}_{j,j'}(\mathbf{t}), \widehat{\boldsymbol{\Sigma}}_j^2(\mathbf{t}), \widehat{\boldsymbol{\Sigma}}_{j'}^2(\mathbf{t}))\}$

8: $\alpha^{(r)} \leftarrow 1$

9: $\sigma_{j,j'}^{(r)} = \alpha^{(r)} \sigma_{j,j'}^{*(r)} + (1 - \alpha^{(r)}) \sigma_{j,j'}^{(r-1)}$

10: $\widetilde{\Sigma}_{j,j'}^{(r-1)} = \widetilde{\Sigma}_{j',j}^{(r-1)} = \sigma_{j,j'}^{(r)}$

11: **while** $\widetilde{\Sigma}_{j,j'}^{(r-1)}$ is not PSD **do**

12: $\alpha^{(r)} \leftarrow \alpha^{(r)} - 0.0001$

13: $\sigma_{j,j'}^{(r)} = \alpha^{(r)} \sigma_{j,j'}^{*(r)} + (1 - \alpha^{(r)}) \sigma_{j,j'}^{(r-1)}$

14: $\widetilde{\Sigma}_{j,j'}^{(r-1)} = \widetilde{\Sigma}_{j',j}^{(r-1)} = \sigma_{j,j'}^{(r)}$

15: $\widetilde{\Sigma}_{j,j'}^{(r)} = \widetilde{\Sigma}_{j',j}^{(r)} = \sigma_{j,j'}^{(r)}$

16: $\alpha_{\text{sum}}^{(r)} \leftarrow \alpha_{\text{sum}}^{(r)} + \alpha^{(r)}$

17: **if** $\alpha_{\text{sum}}^{(r)} / |\mathcal{J}| = 1$ **then** $\epsilon^{(r+1)} \leftarrow 1.1\epsilon^{(r)}$

18: **else if** $\alpha_{\text{sum}}^{(r)} / |\mathcal{J}| < 0.90$ **then** $\epsilon^{(r+1)} \leftarrow 0.9\epsilon^{(r)}$

19: **else if** criterion 1 = True **then** $\epsilon^{(r+1)} \leftarrow 0.5\epsilon^{(r)}$

20: $r \leftarrow r + 1$

21: **end**
Output: $\widehat{\boldsymbol{\Sigma}}$

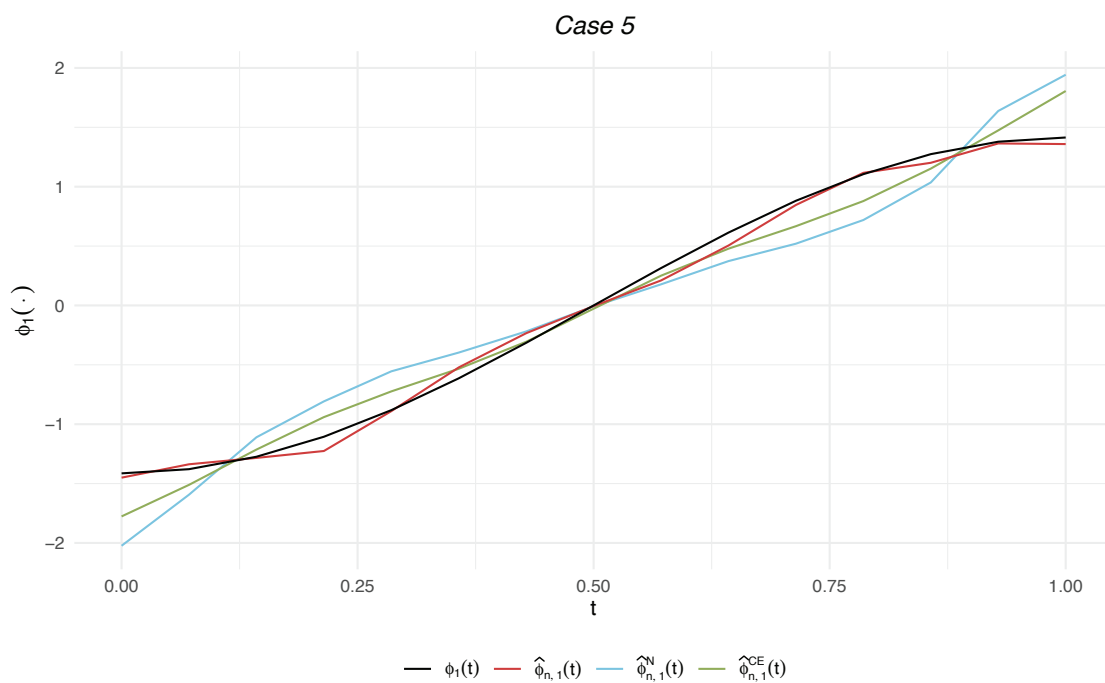


Figure 1: For eigenfunction $\phi_1(t) = -\sqrt{2} \cos(\pi t)$, $\hat{\phi}_1(\cdot)$ is our proposed estimator, $\hat{\phi}_1^N(\cdot)$ is the naïve estimator, and $\hat{\phi}_1^{CE}(\cdot)$ is computed under the canonical PACE method settings.

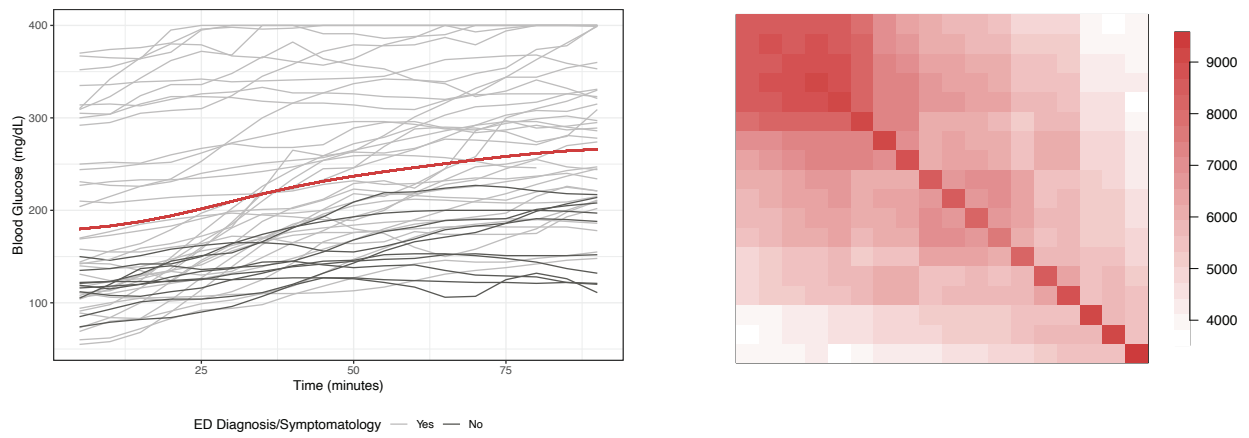


Figure 2: Left: Blood glucose trajectories from the training data (grey) with the estimated mean function (red) overlaid. Right: Estimated covariance surface.

Case	$\hat{\mu}$	$\hat{\mu}^N$	$\mu^{\text{CE}}(\cdot)$	$\hat{\Sigma}(\cdot, \cdot)$	$\hat{\Sigma}^N(\cdot, \cdot)$	$\hat{\Sigma}^{\text{CE}}(\cdot, \cdot)$
<i>Case 1</i>	0.11 (0.01)	0.61 (0.01)	0.67 (0.01)	2.25 (0.04)	2.24 (0.04)	3.79 (0.03)
<i>Case 2</i>	0.14 (0.01)	0.65 (0.01)	0.71 (0.01)	1.68 (0.19)	8.83 (0.07)	8.00 (0.07)
<i>Case 3</i>	0.11 (0.01)	0.63 (0.01)	0.69 (0.01)	1.80 (0.13)	4.08 (0.06)	4.75 (0.05)
<i>Case 4</i>	0.15 (0.01)	0.65 (0.01)	0.71 (0.01)	1.74 (0.19)	8.74 (0.07)	8.00 (0.07)
<i>Case 5</i>	0.04 (0.01)	0.13 (0.01)	0.19 (0.01)	0.16 (0.03)	0.44 (0.02)	0.24 (0.02)

Table 1: SSE for $\hat{\mu}(\cdot)$ and $\hat{\Sigma}(\cdot, \cdot)$, averaged over 100 MC samples. For parameter θ , $\hat{\theta}$ is our proposed estimator, $\hat{\theta}^N$ is the naïve estimator, and $\hat{\theta}^{\text{CE}}$ is computed under the canonical PACE method settings. The MC standard error for each estimator is in parentheses. The best estimator is made bold for each case.

Case	$\widehat{\sigma}^2(\cdot)$	$\widehat{\sigma}^{2,N}(\cdot)$	$\widehat{\sigma}^{2,CE}(\cdot)$	$\widehat{\text{SNR}}$	$\widehat{\text{SNR}}^N$	$\widehat{\text{SNR}}^{CE}$
<i>Case 1</i>	2.59 (0.01)	0.31 (0.01)	0.57 (0.00)	7.08 (0.01)	4.70 (0.03)	13.02 (0.01)
<i>Case 2</i>	0.05 (0.01)	0.02 (0.00)	0.00 (0.00)	0.12 (0.01)	0.30 (0.01)	0.34 (0.01)
<i>Case 3</i>	0.40 (0.01)	0.10 (0.01)	0.12 (0.00)	1.17 (0.02)	1.91 (0.02)	3.84 (0.01)
<i>Case 4</i>	0.05 (0.01)	0.02 (0.00)	0.01 (0.00)	0.13 (0.01)	0.31 (0.01)	0.36 (0.01)
<i>Case 5</i>	0.01 (0.00)	0.01 (0.00)	0.00 (0.00)	0.25 (0.02)	0.36 (0.02)	0.67 (0.01)

Table 2: SSE for $\widehat{\sigma}^2(\cdot)$ and $\widehat{\text{SNR}}$, averaged over 100 MC samples. For parameter θ , $\widehat{\theta}$ is our proposed estimator, $\widehat{\theta}^N$ is the naïve estimator, and $\widehat{\theta}^{CE}$ is computed under the canonical PACE method settings. The MC standard error for each estimator is in parentheses. The best estimator is made bold for each case.